

1

Supplementary Material

2

3 **Single-Atomic Mn Sites of Electronic Configuration** 4 **Regulation mediated by Mo/Mn Clusters for Efficient** 5 **Hydrogen Evolution Reaction**

6

7

8 Chengyu Zhang ^{a,b,c}, Xiangyang Wang ^{a,b,c}, Renyuan Zhao ^{a,b,c}, Fabrice Ndayisenga ^{a,b,c}, Zhisheng
9 Yu ^{a,b,c} *

10

11 ^a College of Resources and Environment, University of Chinese Academy of Sciences, 19 A Yuquan
12 Road, Beijing 100049, P.R. China;

13 ^b Binzhou Institute of Technology, Weiqiao-UCAS Science and Technology Park, Binzhou City
14 256606, Shandong Province, P.R. China;

15 ^c RCEES-IMCAS-UCAS Joint-Lab of Microbial Technology for Environmental Science, Beijing
16 100085, China.

17

18 * Corresponding author.

19 Correspondence should be addressed to Prof. Zhisheng Yu (yuzs@ucas.ac.cn), Tel.: +86-10-
20 88256057; Fax: +86-10-88256057.

21

22 **Text S1 Experimental Procedures**

23 **Electrochemical measurement**

24 The electrochemical research uses a standard three-electrode electrolytic cell with
25 0.5 M H₂SO₄, in which the saturated calomel electrode (SCE) is used as the reference
26 electrode, the graphite rod is used as the counter electrode, and the glass carbon
27 electrode with a diameter of 5 mm is used as the working electrode. All potentials were
28 referenced with a reversible hydrogen electrode (RHE).

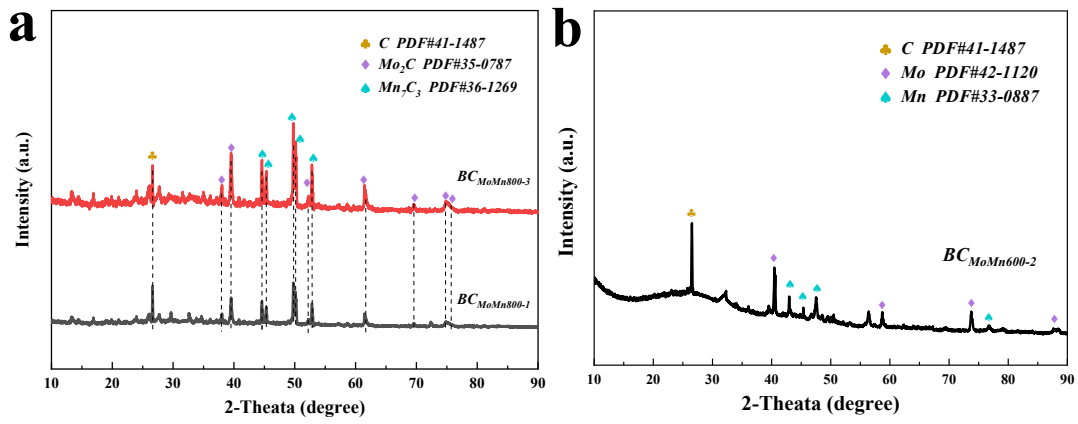
29 5 mg of each catalyst was added 1000 uL anhydrous ethanol and 20 uL Nafion 117
30 solution respectively, and ultrasonic dispersion was carried out for 50 min to form a
31 uniform catalyst ink. 40 uL of the ink was added to the surface of a glassy carbon
32 electrode (5 mm in diameter, superficial area: 0.19625 cm²) and dried under ambient
33 conditions for 4 h. The mass loading on the glassy carbon electrode was 1 mg cm⁻². A
34 commercial Pt (20 wt %) on carbon was used as the reference sample.

35 The HER polarization curve of the catalyst-loaded glassy carbon electrode was
36 obtained by Linear sweep voltammetry (LSV), the potential window was 0 ~ -0.6 V vs.
37 RHE, and at a scan rate of 1 mV s⁻¹. Electrochemical impedance measurements (EIS)
38 were carried out from 100 kHz to 100 mHz and obtained at a current density of 10 mA
39 cm⁻². All subsequent measurements were corrected to an uncompensated resistance of
40 85% of the R_u value. The overpotential of the catalyst was obtained at current densities
41 of 10 mA cm⁻². To estimate the electroactive surface area (ECSA) of the catalyst, we
42 measured cyclic voltammograms between -0.07 ~ -0.17 V vs. RHE at scan rates of 10,
43 20, 40, 80, 120, 160, and 200 mV s⁻¹, respectively. The calculation of the Turnover
44 frequency (TOF) value of the catalyst was based on the equation $TOF = I/2nF$. Where
45 I, n, and F represent the current (A) obtained during the LSV test in 0.5 M H₂SO₄
46 solution, and the active site number of points (mol) and Faraday constant (96485 C mol⁻¹
47 ¹). The number 2 represents the number of moles of electrons consumed to liberate 1
48 mol H₂ from water.

49

50

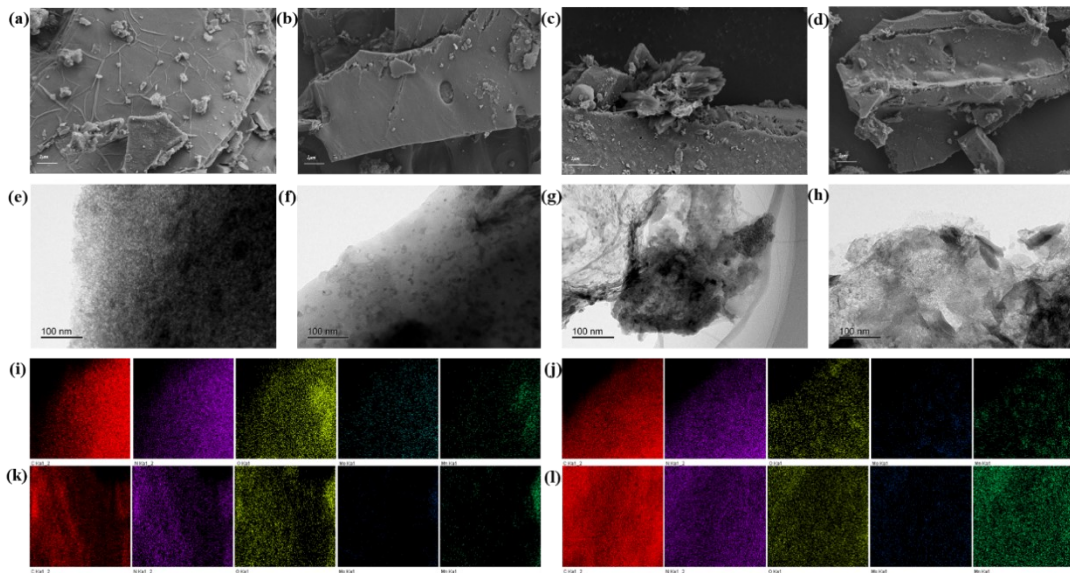
51



52

53

Figure S1. The XRD spectra of a) $BC_{MoMn800-1}$ and $BC_{MoMn800-3}$, b) $BC_{MoMn600-2}$.

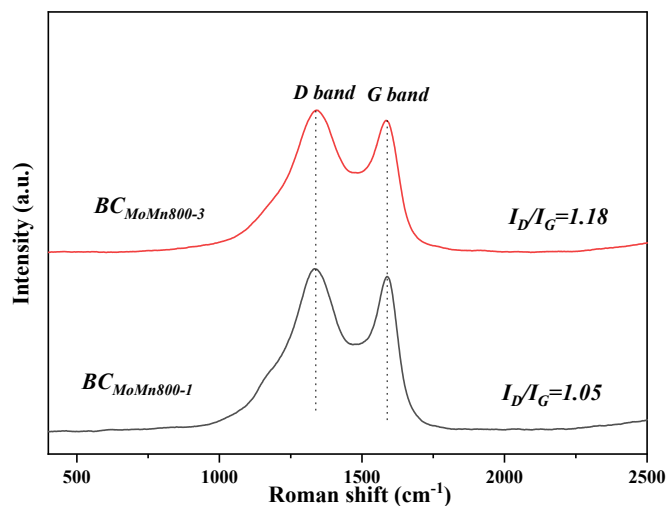


54

55

56

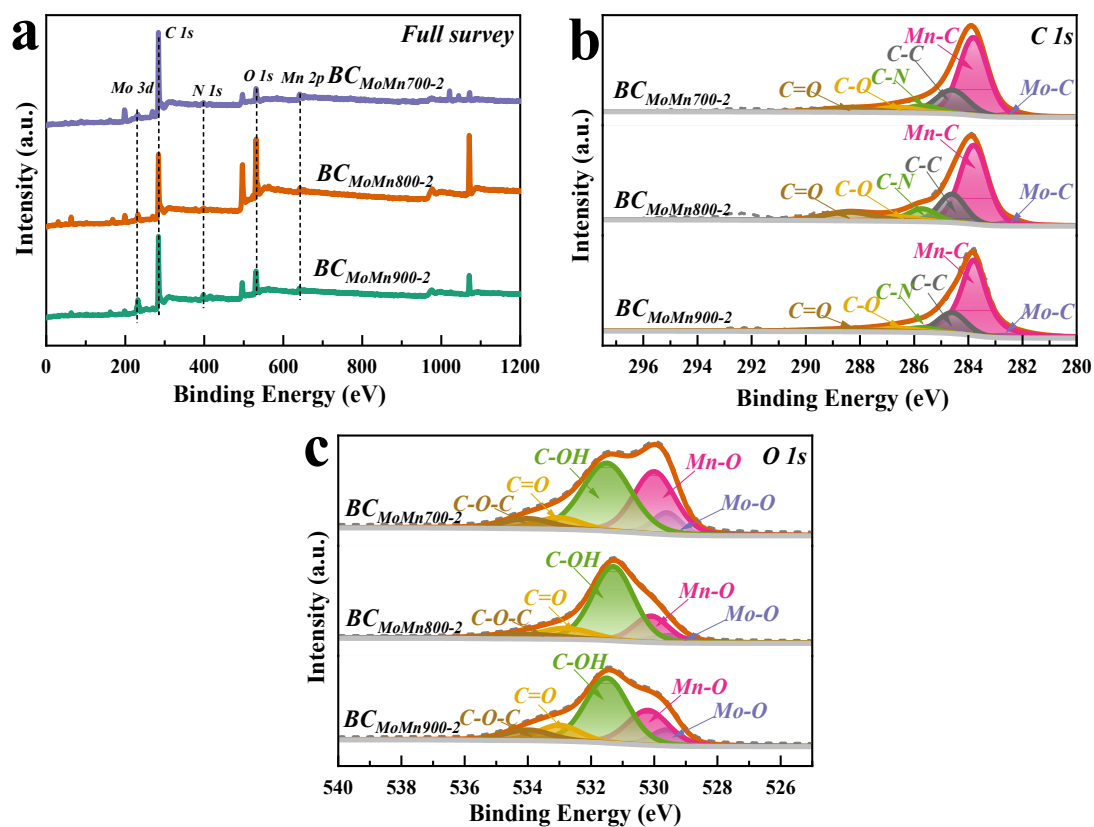
Figure S2. a-d) FESEM, e-h) TEM, and i-l) corresponding EDS line-scan elemental of $BC_{MoMn700-2}$, $BC_{MoMn800-1}$, $BC_{MoMn800-3}$, and $BC_{MoMn900-2}$.



57

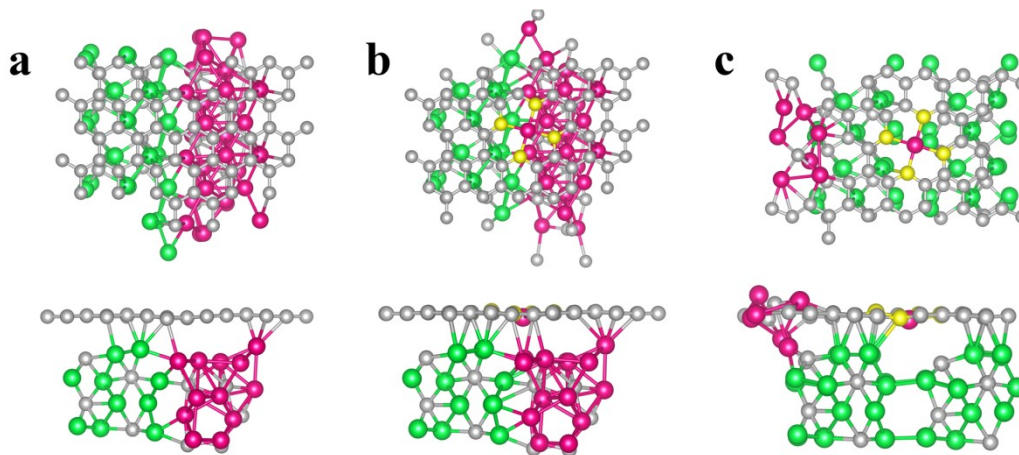
58

Figure S3. The Raman spectra of $BC_{MoMn800-1}$ and $BC_{MoMn800-3}$.



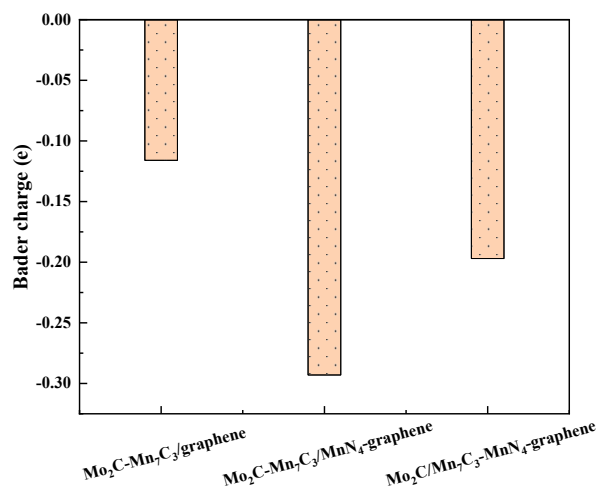
59

60 Figure S4. The a) full survey, b) high-resolution C 1s, and c) O 1s $BC_{MoMn700-2}$, $BC_{MoMn800-2}$, and $BC_{MoMn900-2}$.



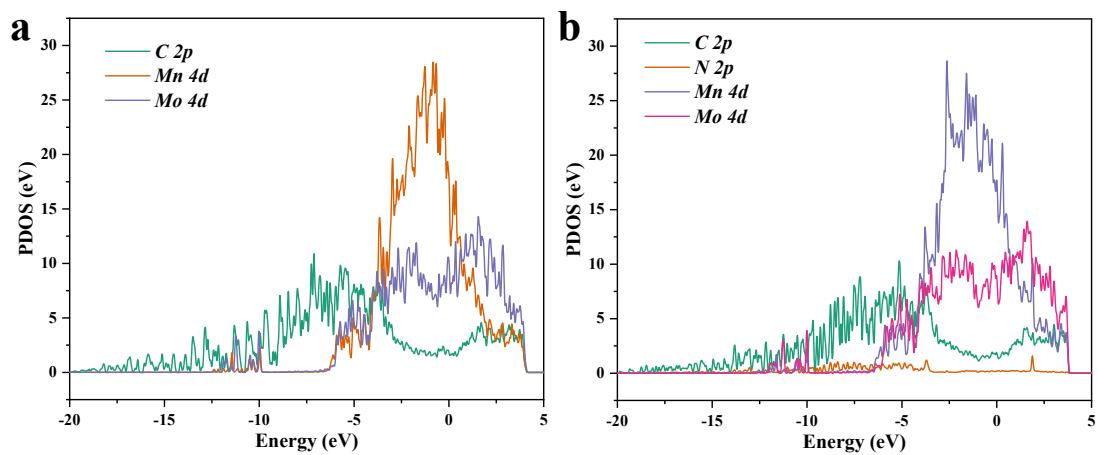
61

62 **Figure S5.** Different views of the optimized structural model. Top and side views of a) $\text{Mo}_2\text{C-Mn}_7\text{C}_3/\text{graphene}$, b)
 63 $\text{Mo}_2\text{C-Mn}_7\text{C}_3/\text{MnN}_4\text{-graphene}$, and c) $\text{Mo}_2\text{C/Mn}_7\text{C}_3\text{-MnN}_4\text{-graphene}$ with H adatom.

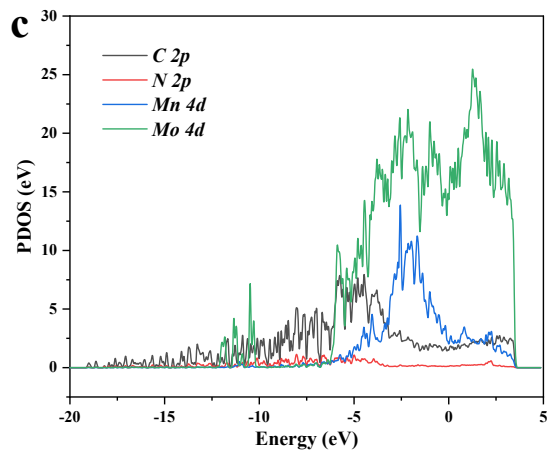


64

65 **Figure S6.** Calculation of Bader charge on $\text{Mo}_2\text{C-Mn}_7\text{C}_3/\text{graphene}$, $\text{Mo}_2\text{C-Mn}_7\text{C}_3/\text{MnN}_4\text{-graphene}$, and
 66 $\text{Mo}_2\text{C/Mn}_7\text{C}_3\text{-MnN}_4\text{-graphene}$.



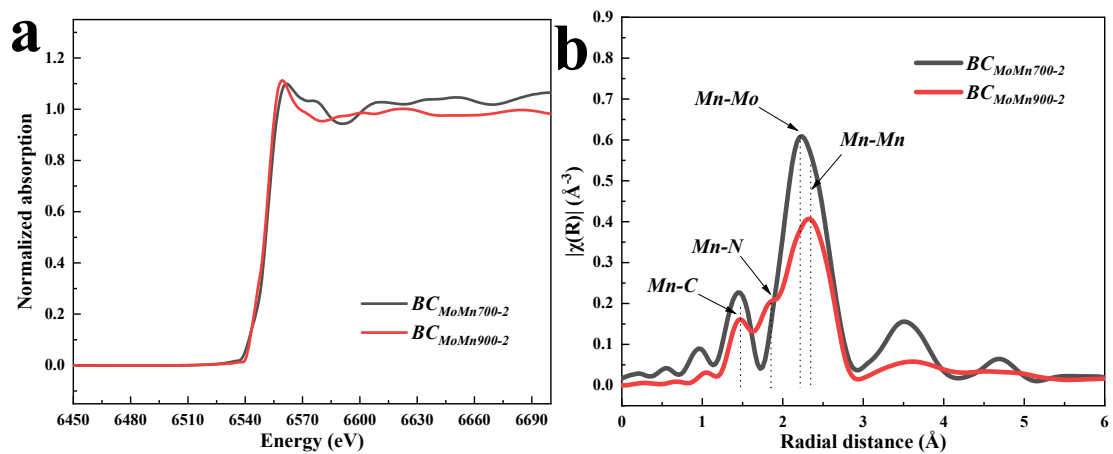
67



68

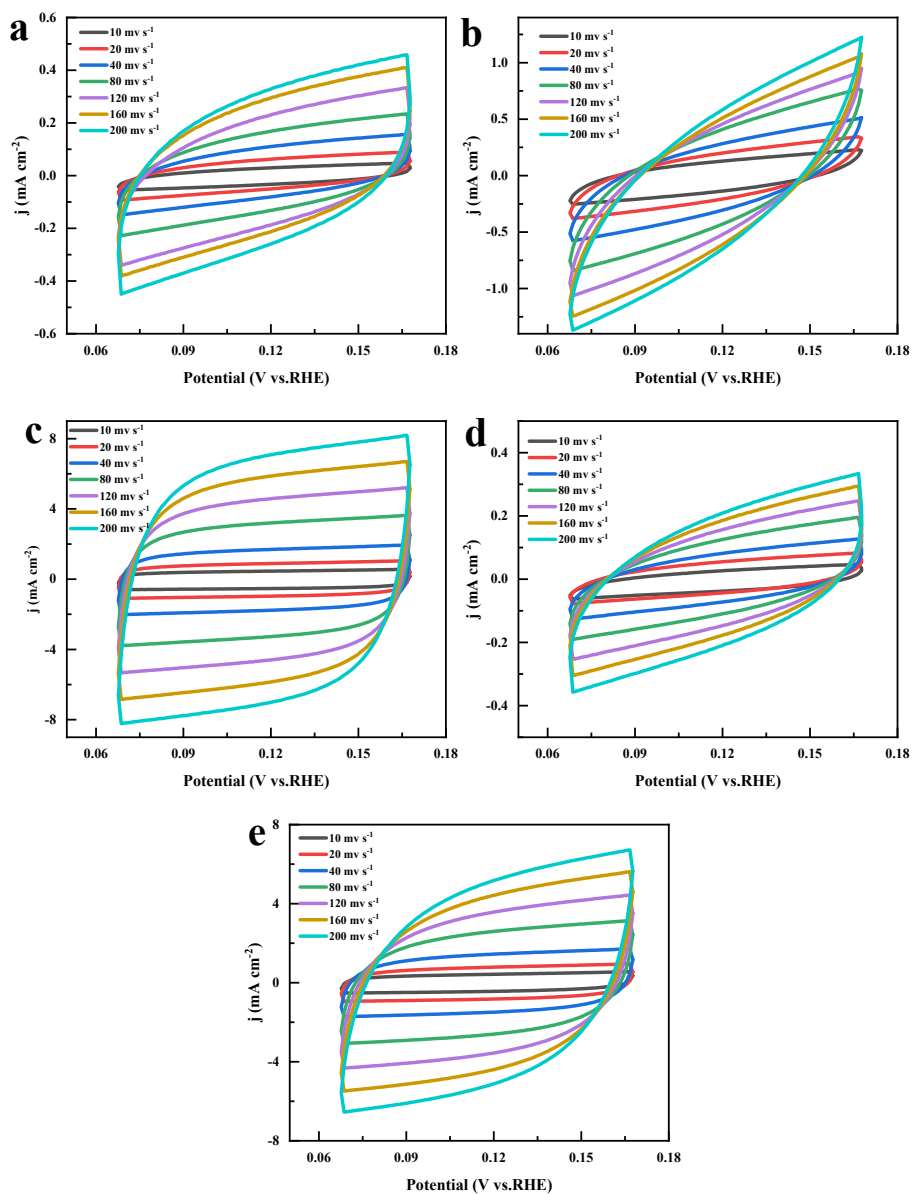
69 **Figure S7.** Density of states of a) $\text{Mo}_2\text{C}-\text{Mn}_7\text{C}_3/\text{graphene}$, b) $\text{Mo}_2\text{C}-\text{Mn}_7\text{C}_3/\text{MnN}_4\text{-graphene}$, and c) $\text{Mo}_2\text{C}/\text{Mn}_7\text{C}_3\text{-MnN}_4\text{-graphene}$ systems.

70



71

72 **Figure S8.** a) Mn K-edge XANES and b) Fourier transforms of EXAFS spectra of $\text{BC}_{\text{MoMn}700-2}$ and $\text{BC}_{\text{MoMn}900-2}$.

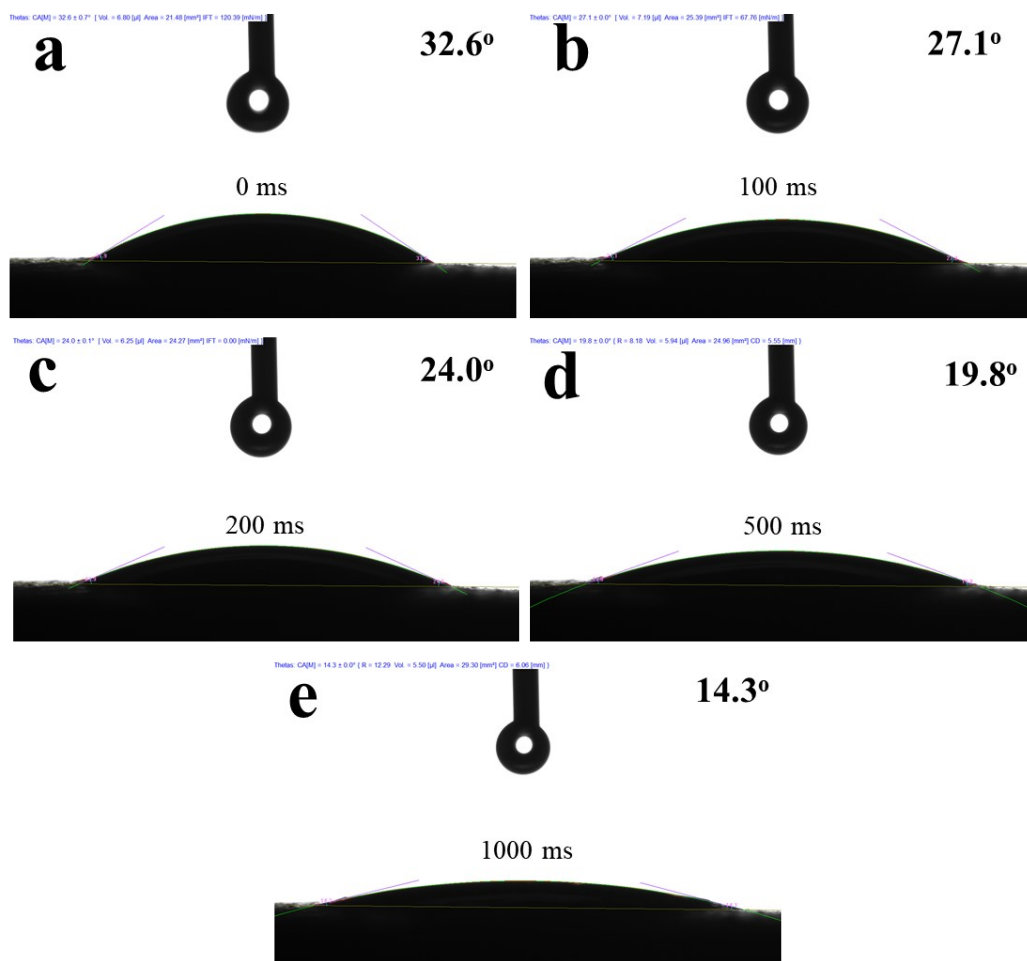


73

74 **Figure S9.** CV curves at different scan rates (10, 20, 40, 80, 120, 160, 200 mV s^{-1}) of a) $\text{BC}_{\text{MoMn700-2}}$, b)

75

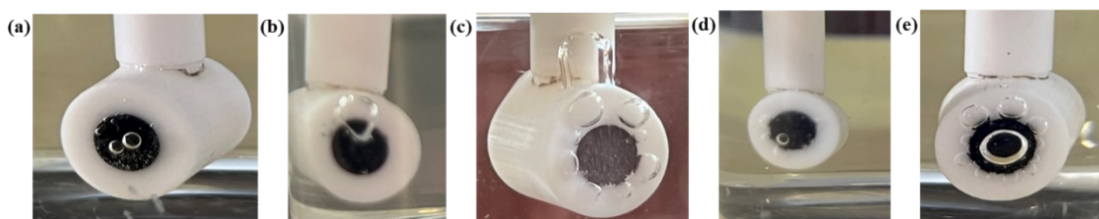
$\text{BC}_{\text{MoMn800-1}}$, c) $\text{BC}_{\text{MoMn800-2}}$, d) $\text{BC}_{\text{MoMn800-3}}$, and e) $\text{BC}_{\text{MoMn900-2}}$.



76

77

Figure S10. Contact angle images between water and electrodes of $BC_{MoMn800-2}$.

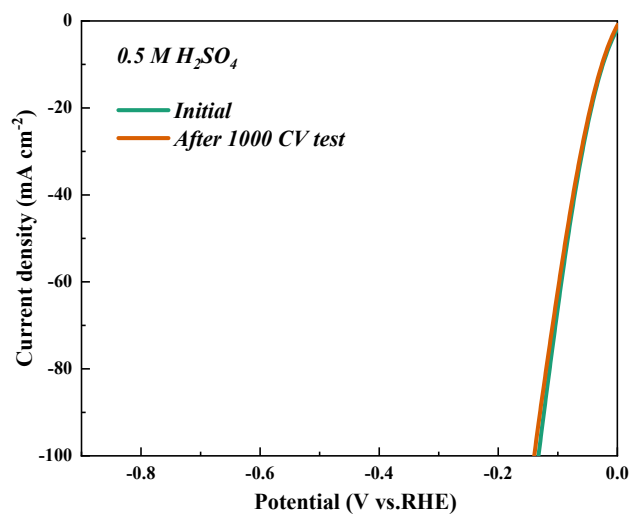


78

Figure S11. A map of the bubbles on the electrode surface. a) $BC_{MoMn700-2}$, b) $BC_{MoMn800-1}$, and c) $BC_{MoMn800-2}$, d)

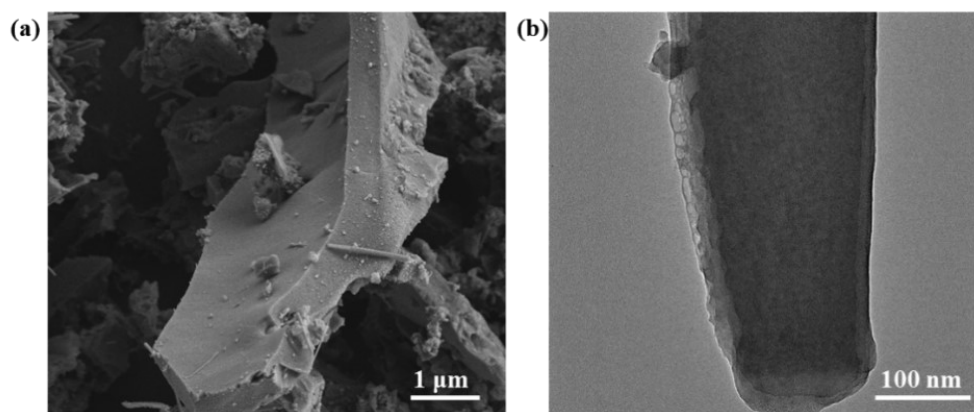
80

$BC_{MoMn800-3}$, e) $BC_{MoMn900-2}$.



81

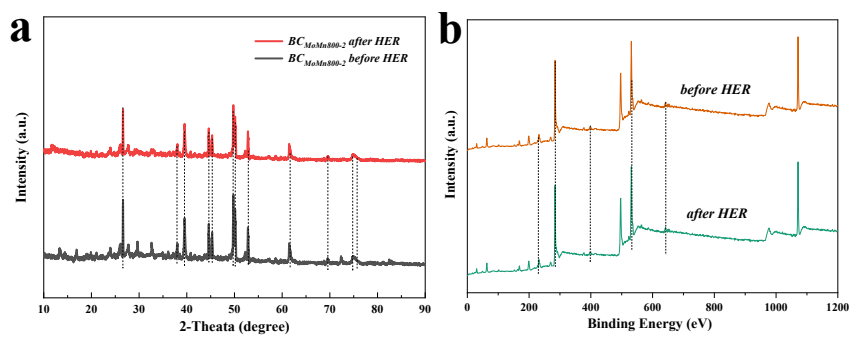
82 **Figure S12.** HER polarization curves of $BC_{MoMn800-2}$ after 1000 CV cycles test at the scan rate of 100 mV s^{-1} .



83

84

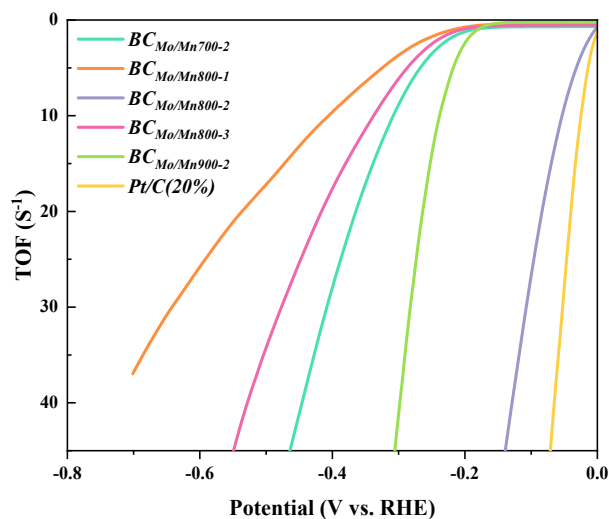
Figure S13. SEM and TEM images of $BC_{MoMn800-2}$ after CV tests.



85

86

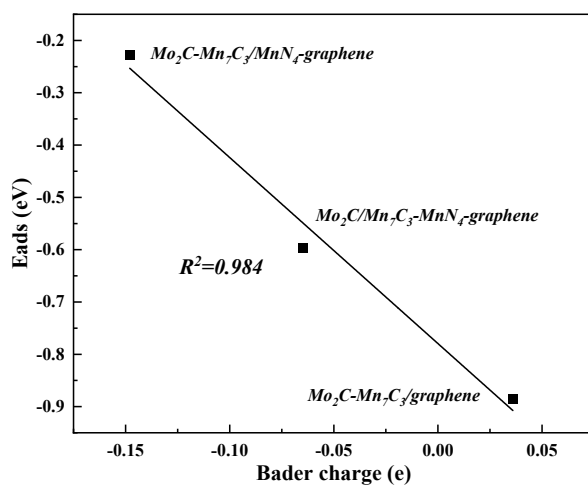
Figure S14. XRD and XPS spectra of $BC_{MoMn800-2}$ after CV tests.



87

88

Figure S15. TOF curves of $BC_{MoMn700-2}$, $BC_{MoMn800-1}$, $BC_{MoMn800-2}$, $BC_{MoMn800-3}$ and $BC_{MoMn900-2}$.



89

90

91

92

Figure S16. The correlation of atomic H adsorption energy with the charge transfer. R^2 , coefficient of determination.

93 **Table S1**94 **Table S1** The content of Mo and Mn elements were detected by ICP-OES.

Samples	The content of Mo element in the samples (wt%)	The content of Mn element in the samples (wt%)
BC _{MoMn700-2}	4.12	6.15
BC _{MoMn800-1}	4.41	3.86
BC _{MoMn800-2}	6.53	8.61
BC _{MoMn800-3}	9.79	11.21
BC _{MoMn900-2}	8.58	10.93

95

96

97 **Table S2**98 **Table S2** Quantitative analysis of functional groups in XPS spectra.99 **N 1s**

Sample	Surface functional group	Group content on the surface
		(at.%)
BC _{MoMn700-2}	oxidized-N	39.6
	graphitic-N	27.7
	pyrrolic-N	15.0
	pyridinic-N	17.7
BC _{MoMn800-2}	oxidized-N	24.2
	graphitic-N	42.6
	Mn-N	21.4
	pyridinic-N	11.8
BC _{MoMn900-2}	oxidized-N	14.4
	graphitic-N	41.4
	Mn-N	19.9
	pyridinic-N	24.3

100 **Mo 3d**

Sample	Surface functional group	Group content on the surface
		(at.%)
BC _{MoMn700-2}	Mo ²⁺	57.2
	Mo ⁴⁺	16.6
	Mo ⁶⁺	26.2
BC _{MoMn800-2}	Mo ²⁺	51.3
	Mo ⁴⁺	28.2
	Mo ⁶⁺	20.5
BC _{MoMn900-2}	Mo ²⁺	24.4

	Mo ⁴⁺	54.4
	Mo ⁶⁺	21.2

101 **Mn 2p**

Sample	Surface functional group	Group content on the surface (at.%)
BC _{MoMn700-2}	Mn ²⁺	41.6
	Mn ³⁺	58.4
BC _{MoMn800-2}	Mn ²⁺	47.7
	Mn ³⁺	52.3
BC _{MoMn900-2}	Mn ²⁺	55.0
	Mn ³⁺	45.0

102